Electronic Supplementary Material (ESI) for Journal of Materials Chemistry A.

Supporting Information

A Multi-Shelled V_2O_3/C Composite with Overall Coupled Carbon Scaffold Enabling Ultrafast and Stable Lithium/Sodium Storage

Yutong Li,[a] Su Zhang,[b] Shitong Wang,[a, c] Jin Leng,[a] Caihua Jiang,[a] Xiaowei Ren,[a] Zhongtai Zhang,[a] Yong Yang,*[, d] Zilong Tang,*[, a]

a. *State Key Lab of New Ceramics and Fine Processing, School of Materials Science and Engineering, Tsinghua University, Beijing 100084, China*
E-mail: tzl@tsinghua.edu.cn

b. *Key Laboratory of Energy Materials Chemistry, Ministry of Education; Key Laboratory of Advanced Functional Materials, Autonomous Region; Institute of Applied Chemistry, Xinjiang University, Urumqi, 830046, P. R. China.*

c. *Department of Nuclear Science and Engineering, Massachusetts Institute of Technology, Cambridge, Massachusetts 02139, USA*

d. *State Key Laboratory of Solidification Processing Center of Advanced Lubrication and Seal Materials, Northwestern Polytechnical University, Xi'an, Shanxi 710072, P. R. China*
E-mail: yongyangfj@nwpu.edu.cn

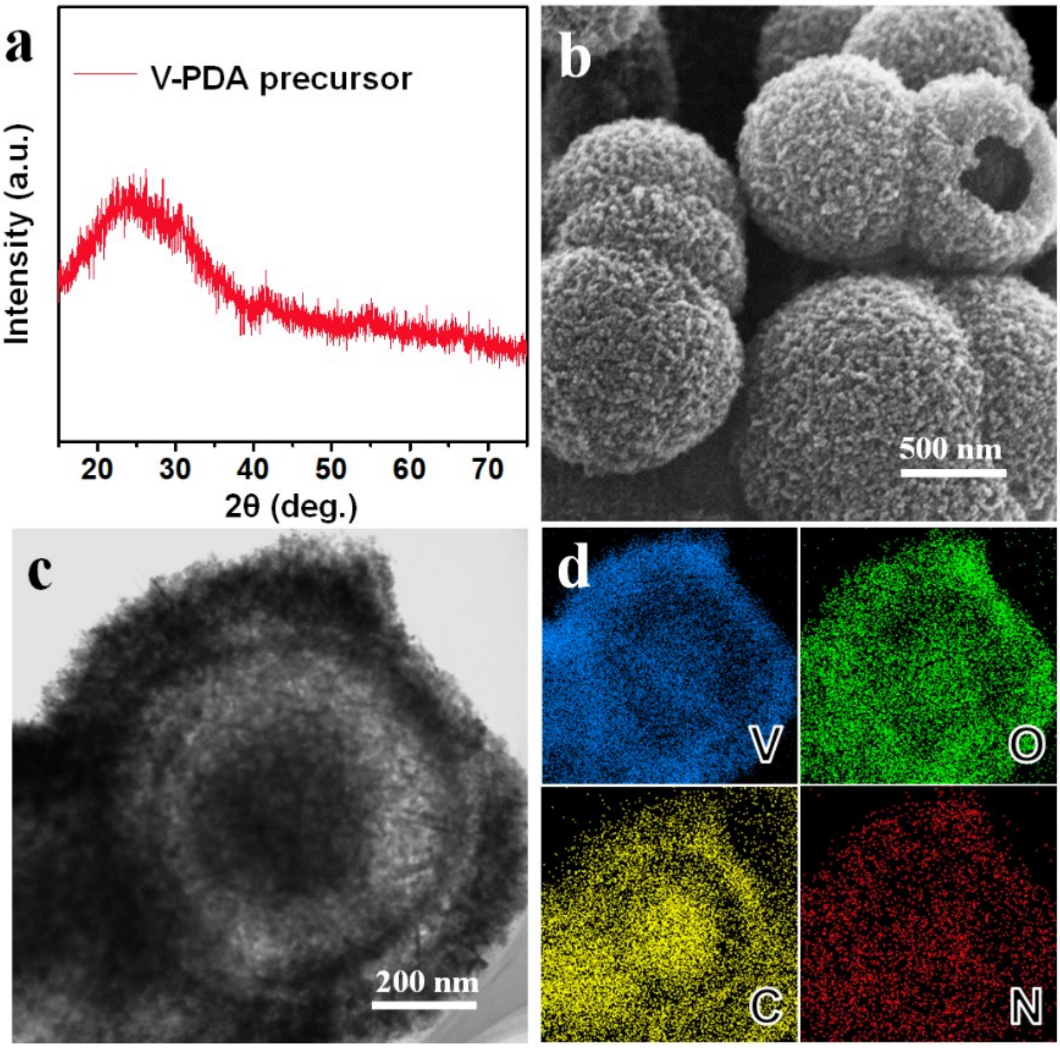

Figure S1. a) XRD pattern, b) SEM image, c) TEM image and d) EDS mapping of the multi-shelled V-PDA precusor.

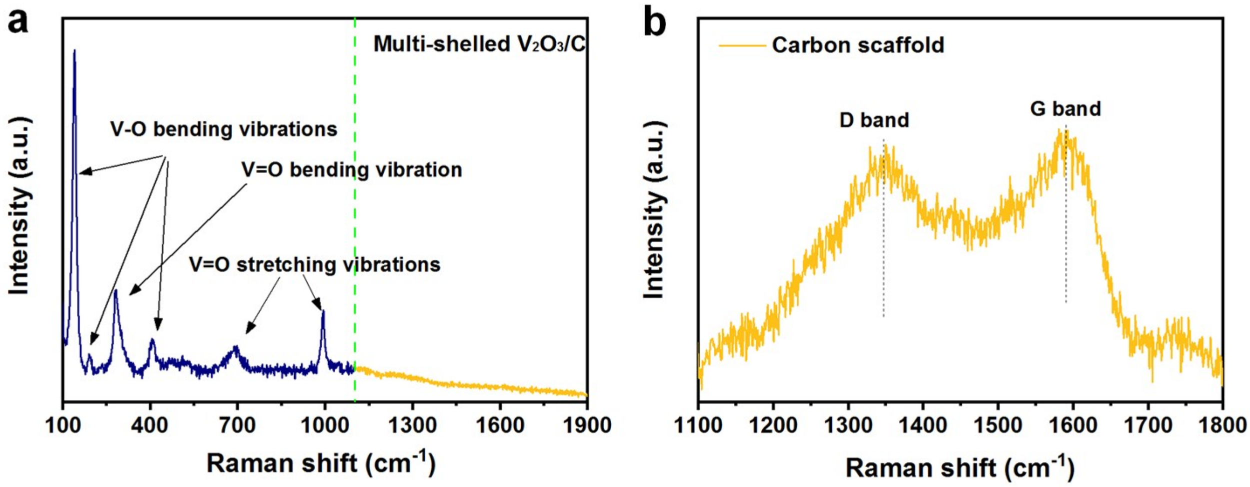

Figure S2. Raman spectra of a) the multi-shelled V_2O_3/C composite and b) the multi-shelled carbon scaffold.

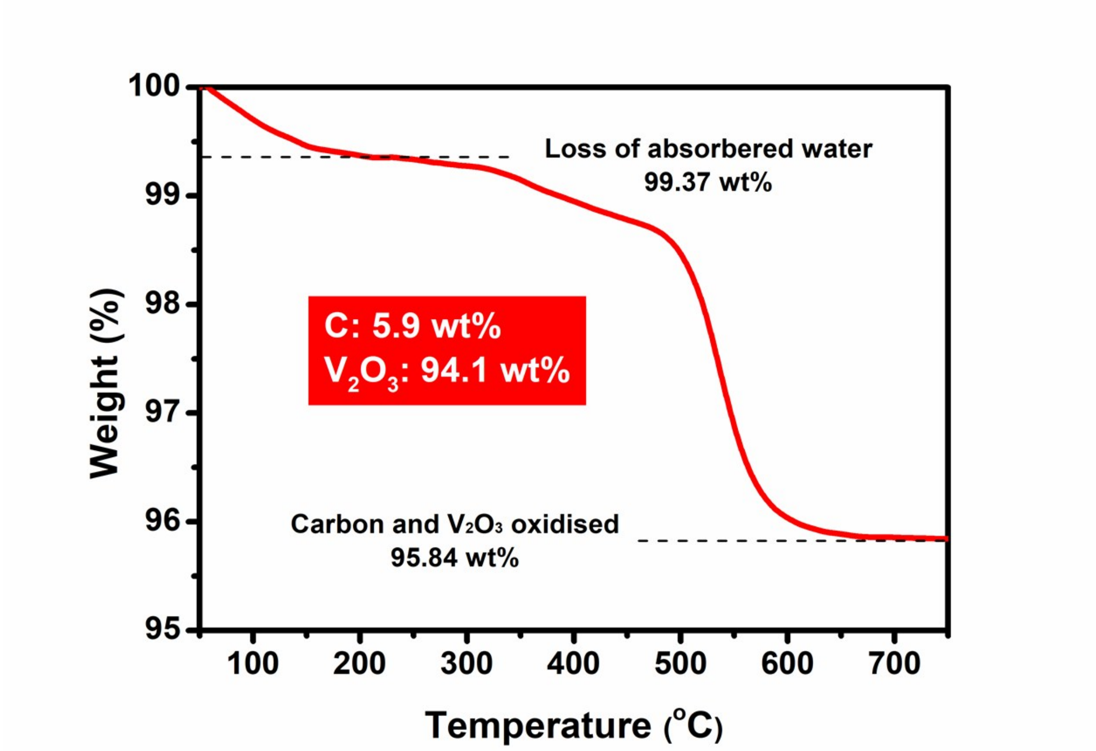

Figure S3. TGA curve of the multi-shelled V_2O_3/C composite.

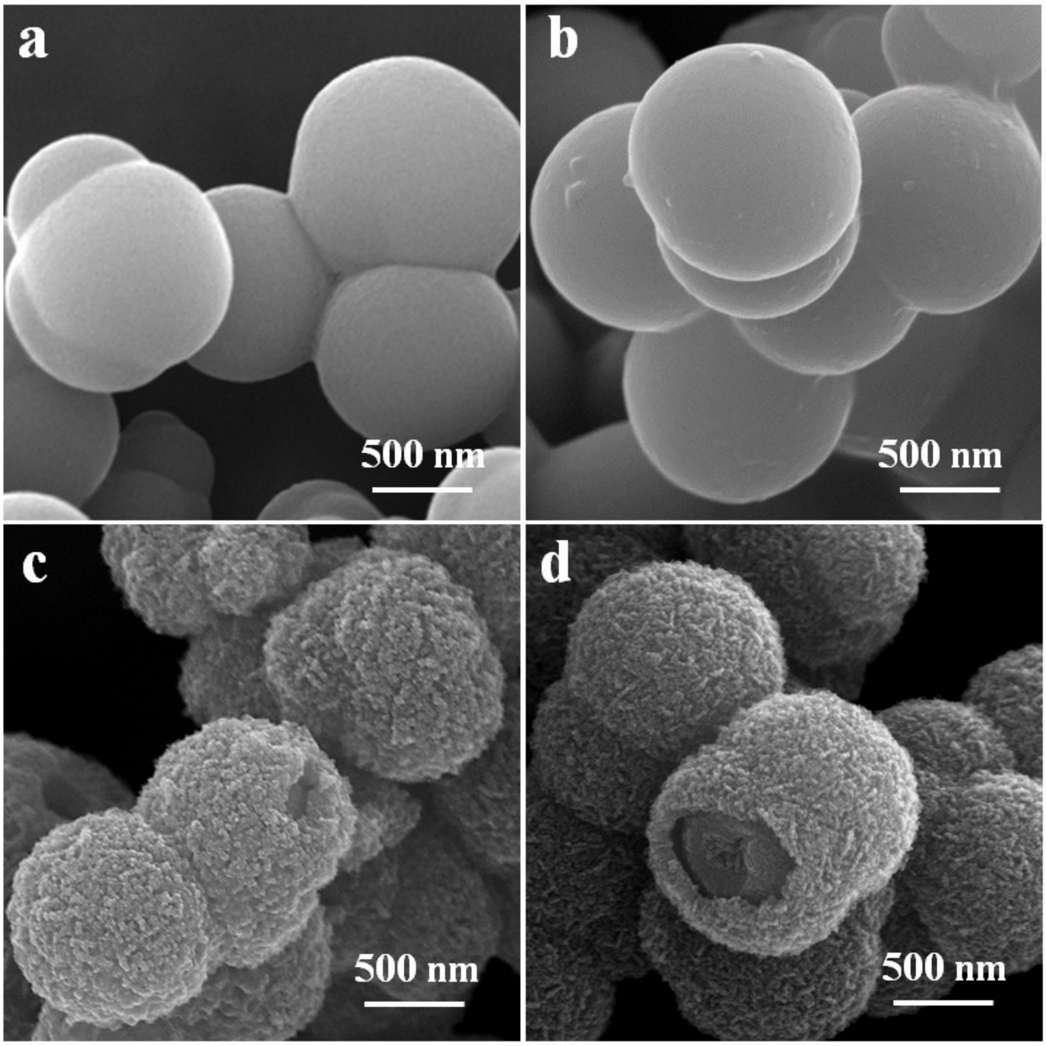

Figure S4. SEM images of V-PDA precusors with different solvothermal durations. a) V-PDA-3h. b) V-PDA-6h. c) V-PDA-9h. d) V-PDA-20h.

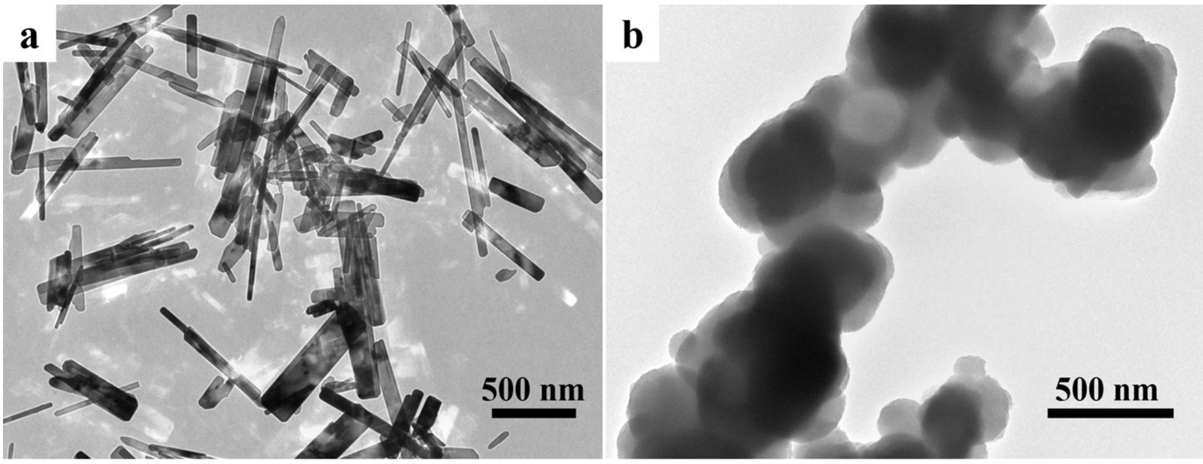

Figure S5. a) TEM image of V_2O_3 nanoflakes prepared without adding dopamine hydrochloride. b) TEM image of polydopamine spheres obtained without adding vanadium salt.

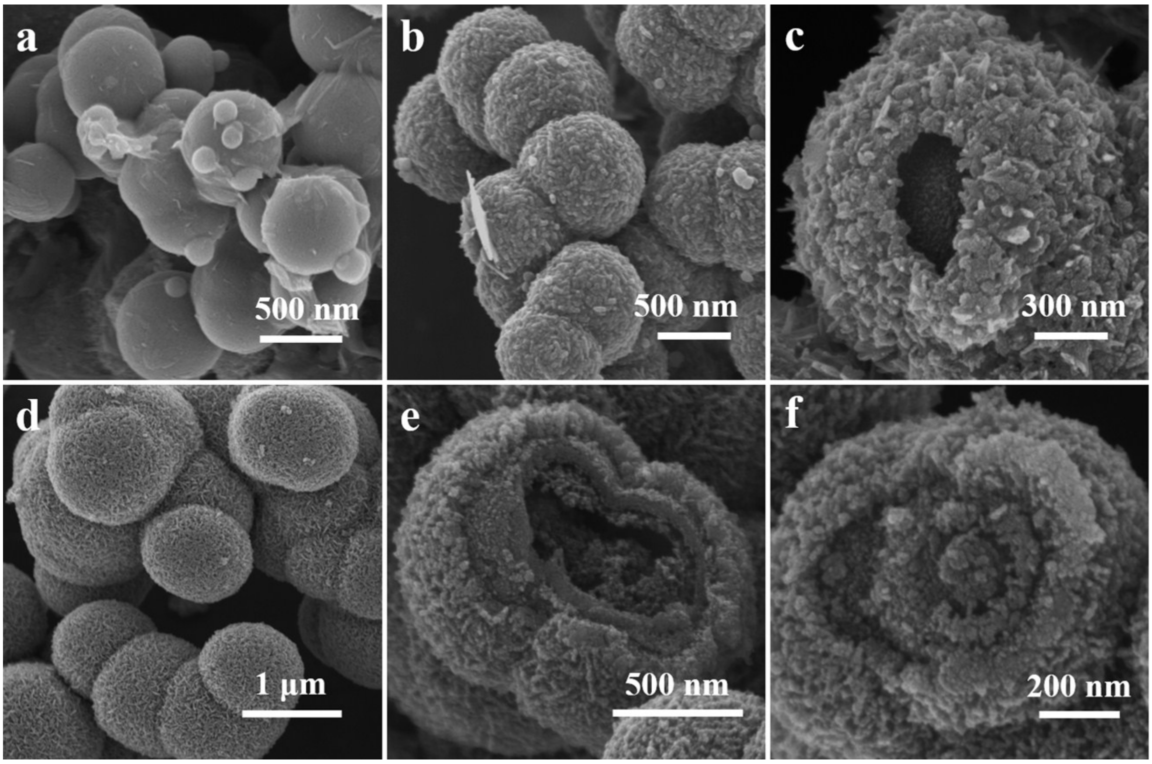

Figure S6. SEM images of a) solid, b-c) double-shelled, and d-f) multi-shelled V_2O_3/C composites.

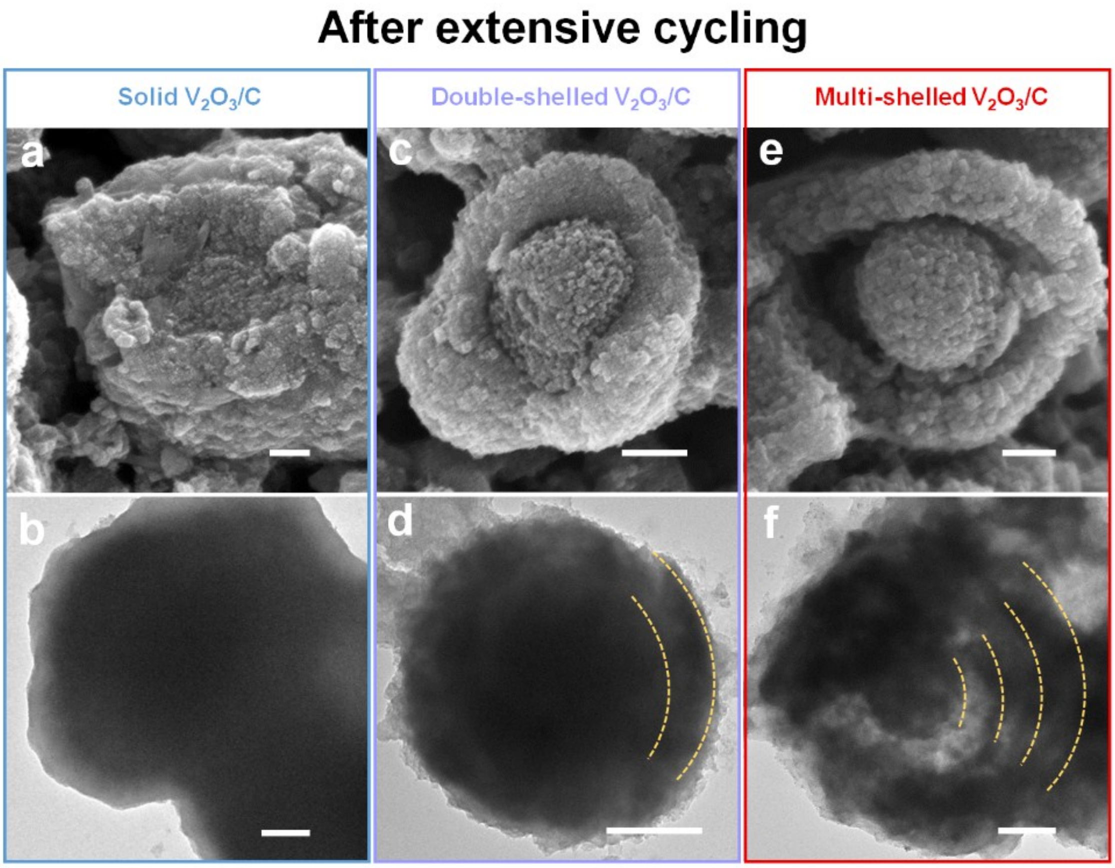

Figure S7. SEM images and TEM images of a-b) solid, c-d) double-shelled, and e-f) multi-shelled V_2O_3/C electrodes after 1500 cycles under 1000 mA g^{-1} current density. The scale bars are 200 nm.

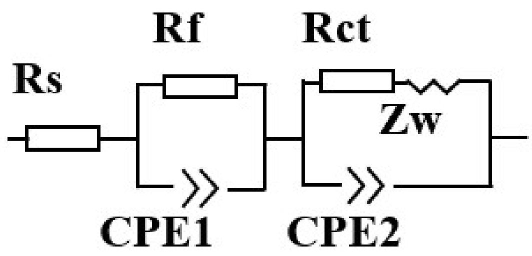

Figure S8. Equivalent circuit model using for fitting EIS spectra.

Table S1. EIS fitting results according to the equivalent circuit model shown in Figure S8.

Samples	R_s (Ω)	R_f (Ω)	R_{ct} (Ω)
Solid V_2O_3/C	2.1		324.4
Double-shelled V_2O_3/C	1.7		234.0
Multi-shelled V_2O_3/C	2.6		102.8
Multi-shelled V_2O_3/C after 100 cycles	4.3	22.1	41.4

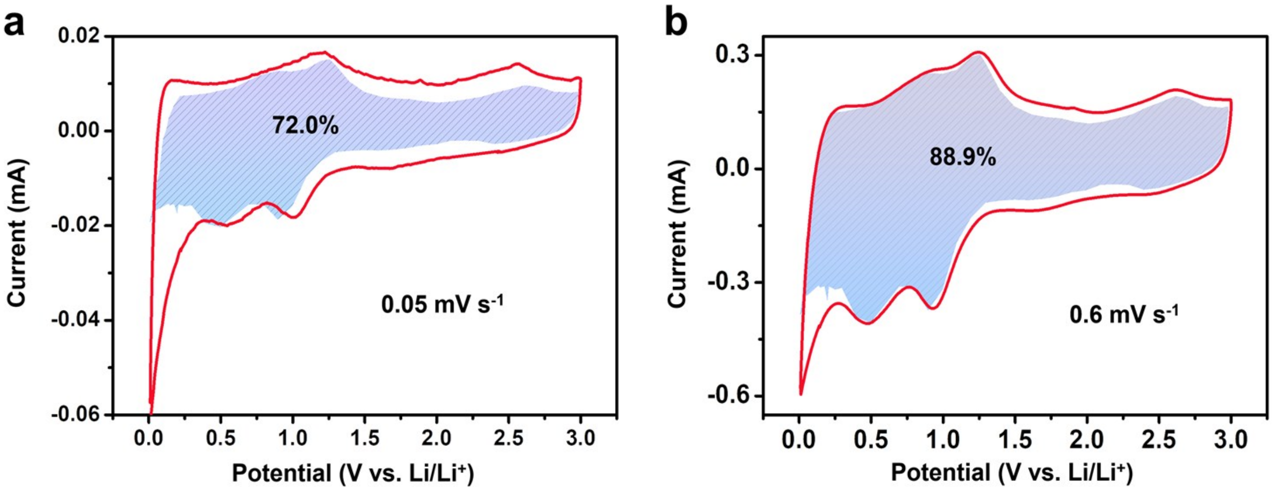

Figure S9. Capacitive-contributed to lithium storage of the multi-shelled V_2O_3/C electrode at a) 0.05 mV s^{-1} and b) 0.6 mV s^{-1}.

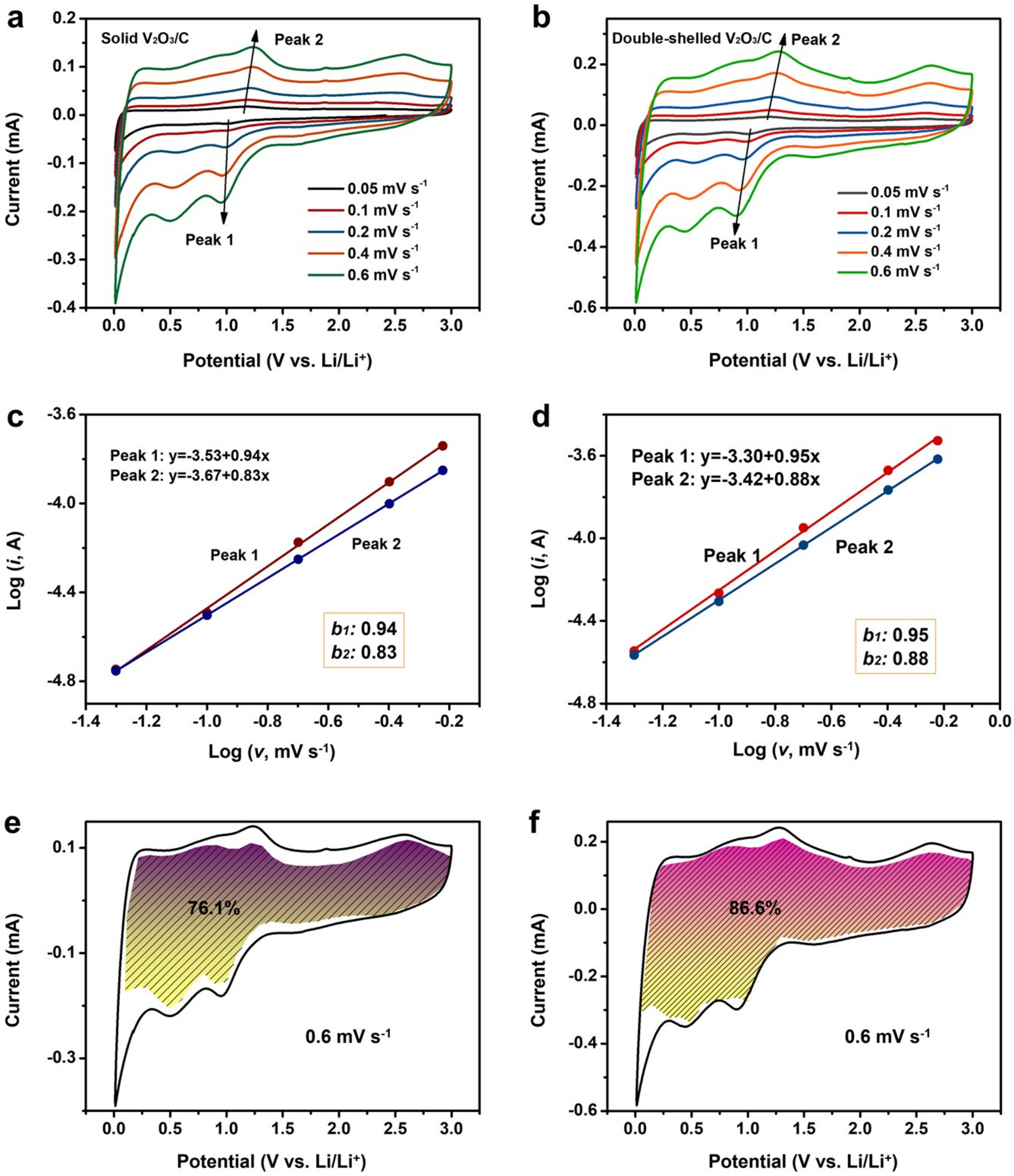

Figure S10. CV curves of a) the solid and b) the double-shelled V_2O_3/C electrodes at different scan rates. Corresponding log(v)-log(i) linear relationship of c) the solid and d) the double-shelled V_2O_3/C electrodes. Capacitive-contributed to charge storage at 0.6 mV s^{-1} of e) the solid and f) the double-shelled V_2O_3/C electrodes.

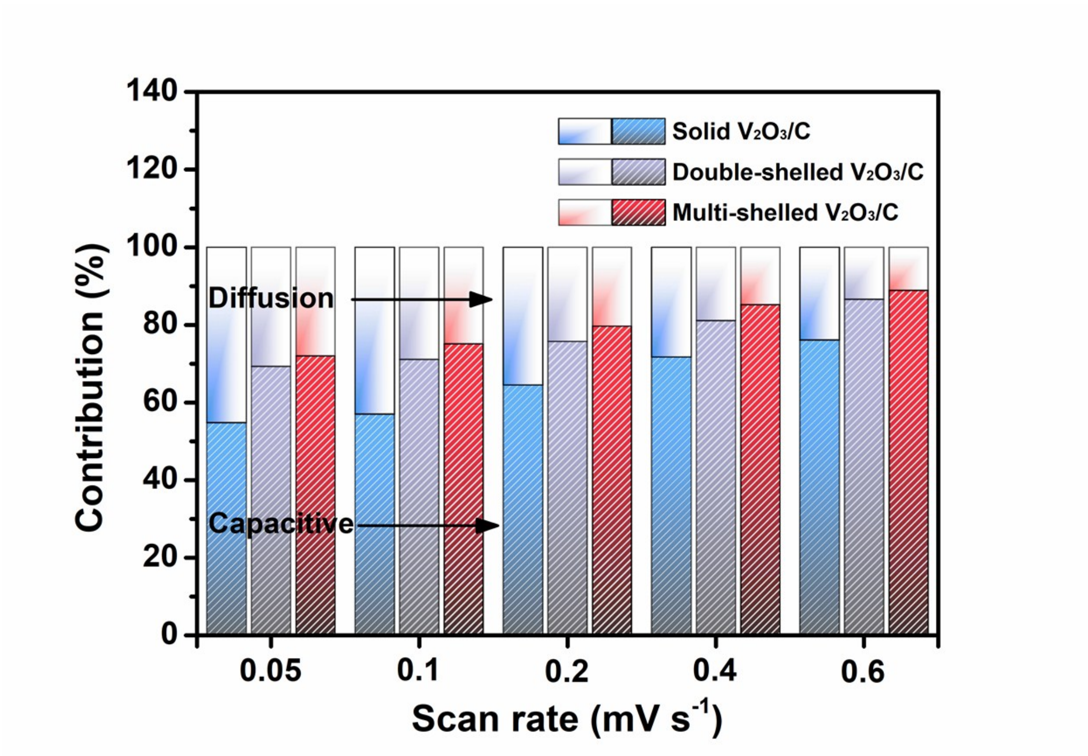

Figure S11. Normalized ratio comparison of diffusion and capactive-controlled capacities calculated at different scan rates for solid, double-shelled and multi-shelled V_2O_3/C electrodes in LIBs.

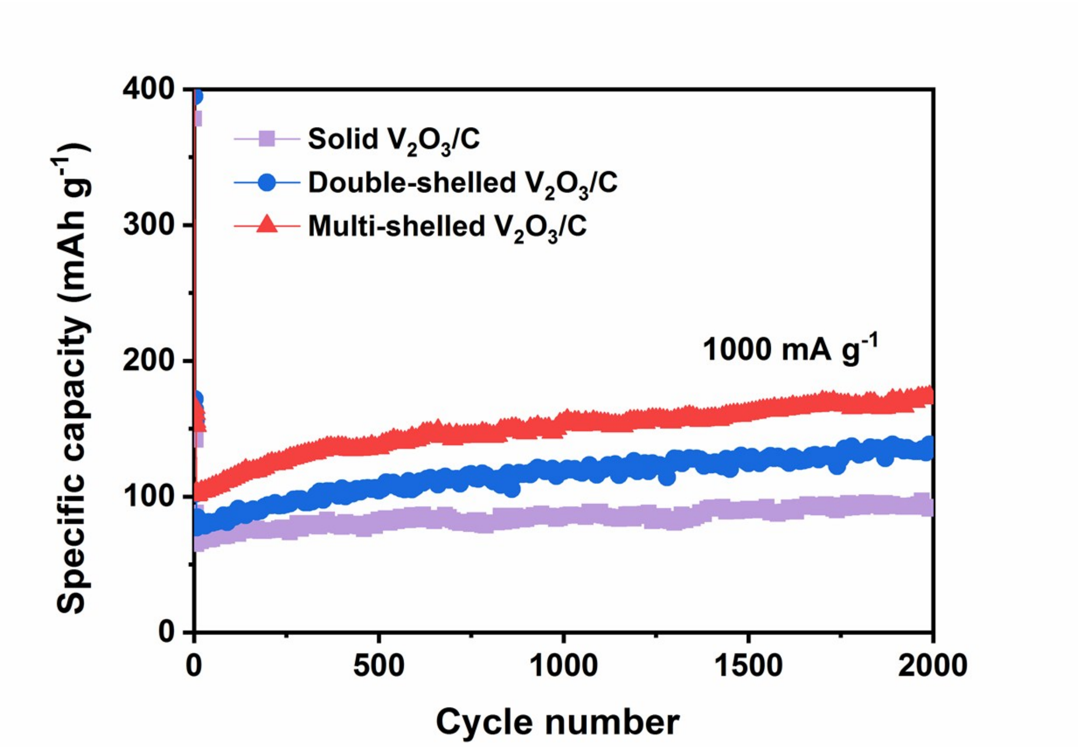

Figure S12. Cycling performance of the solid, double-shelled, and multi-shelled V_2O_3/C composites for SIBs.

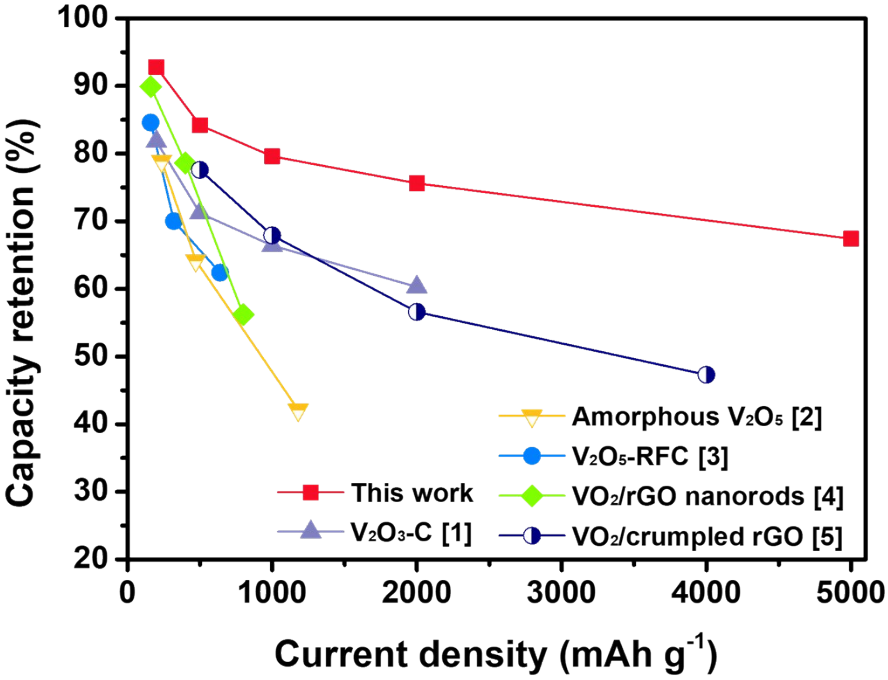

Figure S13. Comparison of the capacity retention in SIBs for multi-shelled V_2O_3 and other vanadium oxide-based anodes.

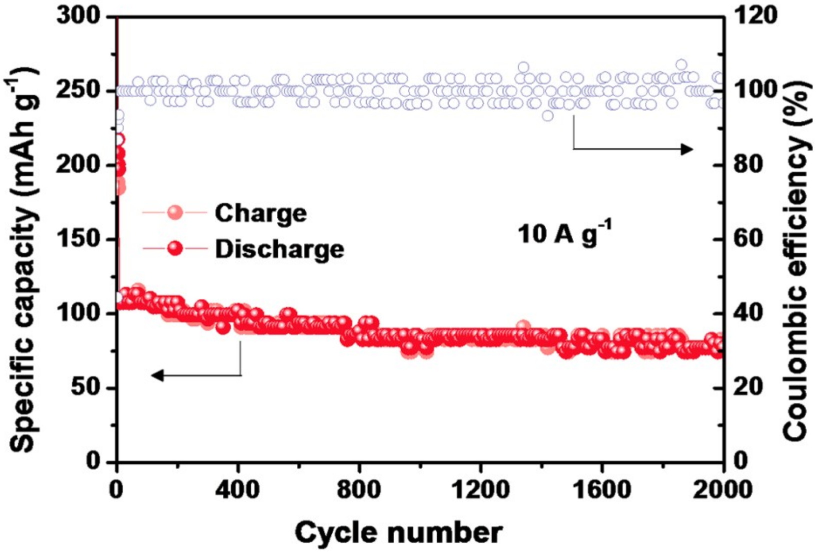

Figure S14. Cycling performance of the multi-shelled V_2O_3/C at 10 A g^{-1}.

Table S2. Comparison of long-term cycling stability in SIBs for multi-shelled V_2O_3 and reported vanadium oxide-based anodes.

Materials	Reversible capacity	Decay rate per cycle	Reference
Multi-shelled V_2O_3/C	79 mAh g^{-1} at 10 A g^{-1} after 2000 cycles	0.013%	This work
	173 mAh g^{-1} at 1 A g^{-1} after 2000 cycles	No decay	
V_2O_3-C	123 mAh g^{-1} at 2 A g^{-1} after 1000 cycles	0.032%	[1]
Amorphous V_2O_5	140 mAh g^{-1} at 23.6 mA g^{-1} after 100 cycles	0.420%	[2]
V_2O_5-RFC	150 mAh g^{-1} at 40 mA g^{-1} after 70 cycles	0.357%	[3]
VO_2/rGO nanorods	173 mAh g^{-1} at 60 mA g^{-1} after 100 cycles	0.300%	[4]
VO_2/crumpled rGO	157 mAh g^{-1} at 4 A g^{-1} after 2000 cycles	0.013%	[5]
Bilayer V_2O_5	200 mAh g^{-1} at 20 mA g^{-1} after 320 cycles	0.167%	[6]
TMC/V_2O_5	51 mAh g^{-1} at 1.07 A g^{-1} after 2000 cycles	0.013%	[7]
GQDs-coated VO_2	227 mAh g^{-1} at 1.5 A g^{-1} after 500 cycles	0.018%	[8]
V_2O_3/KB carbon	ca. 140 mAh g^{-1} at 1 A g^{-1} after 1000 cycles	ca. 0.060%	[9]

References

1 Y. S. Cai, G. Z. Fang, J. Zhou, S. N. Liu, Z. G. Luo, A. Q. Pan, G. Z. Cao and S. Q. Liang, Nano Res. 2018, **11**, 449.

2 E. Uchaker, Y. Z. Zheng, S. Li, S. L. Candelaria, S. Hu and G. Z. Cao, J. Mater. Chem. A 2014, **2**, 18208.

3 V. Raju, J. Rains, C. Gates, W. Luo, X. F. Wang, W. F. Stickle, G. D. Stucky and X. L. Ji, Nano Lett. 2014, **14**, 4119.

4 G. He, L. J. L and A. Manthiram, J. Mater. Chem. A 2015, **3**, 14750.

5 B. Yan, X. F. Li, Z. M. Bai, L. X. Lin, G. Chen, X. S. Song, D. B. Xiong, D. J. Li and X. L. Sun, J. Mater. Chem. A 2017, **5**, 4850.

6 S. Tepavcevic, H. Xiong, V. R. Stamenkovic, X. B. Zuo, M. Balasubramanian, V. B. Prakepenka, C. S. Johnson and T. Rajh, ACS Nano 2012, **6**, 530.

7 S. Fleischmann, D. Leistenschneider, V. Lemkova, B. Krüner, M. Zeiger, L. Borchardt and V. Presser, Chem. Mater. 2017, **29**, 8653.

8 D. L. Chao, C. R. Zhu, X. H. Xia, J. L. Liu, X. Zhang, J. Wang, P. Liang, J. Y. Lin, H. Zhang, Z. X. Shen and H. J. Fan, Nano Lett. 2015, **15**, 565.

9 X. X. An, H. L. Yang, Y. P. Wang, Y. Tang, S. Q. Liang, A. Q. Pan, G. Z. Cao, Sci. China Mater. 2017, **60**, 717.